

Supporting Information

Design of Porous Ag Platelet Structures with Tuneable Porosity and Highly Catalytic Activity

Man Xu,^a Yongming Sui,^{*a} Chao Wang,^a Bo Zhou,^a Yingjin Wei,^b and Bo Zou^{*a}

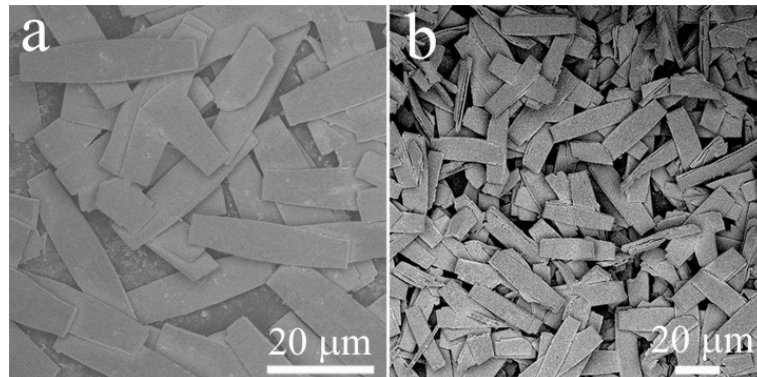


Figure S1. Low-magnification FE-SEM images of a) the precursors and b) the FPP Ag (I) structures.

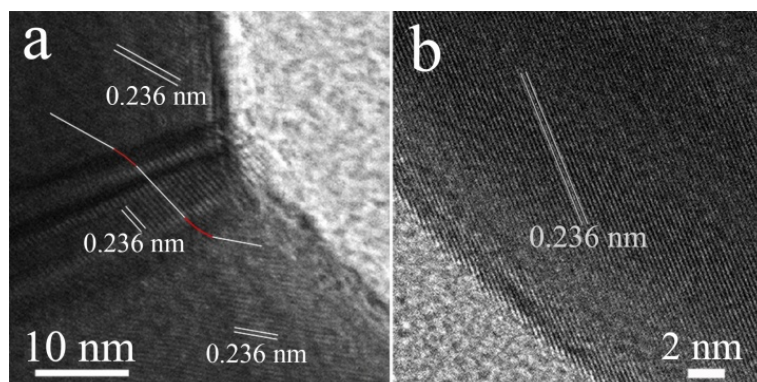


Figure S2. HR-TEM images of the FPP Ag (I) structures.

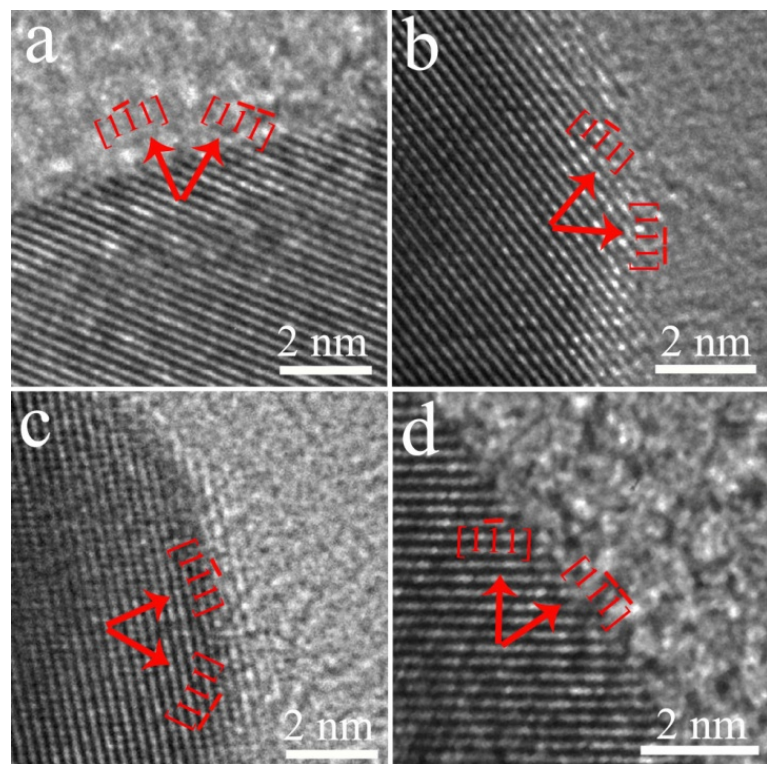


Figure S3. HR-TEM images of the porosity edge in the FPP Ag (I) structures.

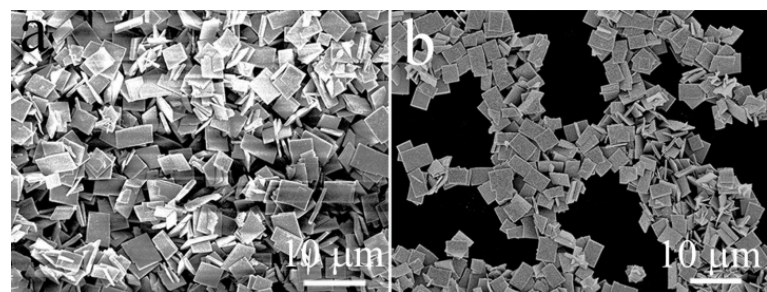


Figure S4. FE-SEM images of a) the precursors and b) the QPP Ag (I) structures.

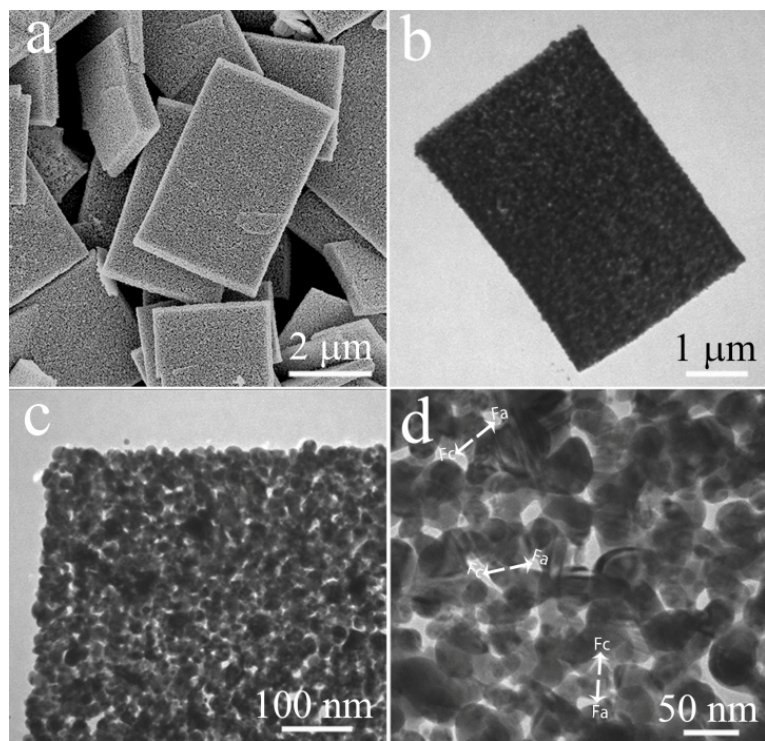


Figure S5. a) High-magnification FE-SEM image b) TEM image and c, d) high-magnification TEM images of the QPP Ag (I) structures.

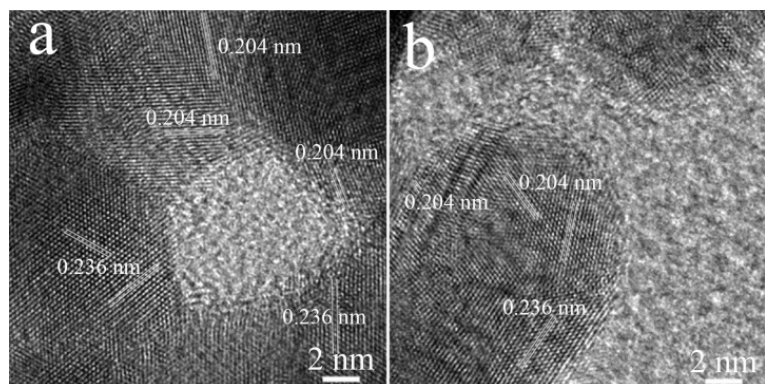


Figure S6. HRTEM images of the QPP Ag (I) structures.

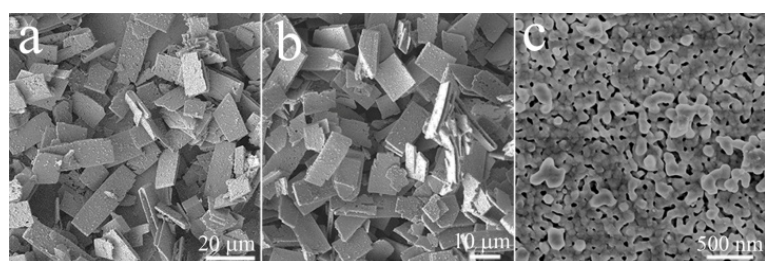


Figure S7. FE-SEM and high-magnification FE-SEM images of a) the precursors, and b, c) FPP Ag (II) structures synthesized at pH= 7.1.

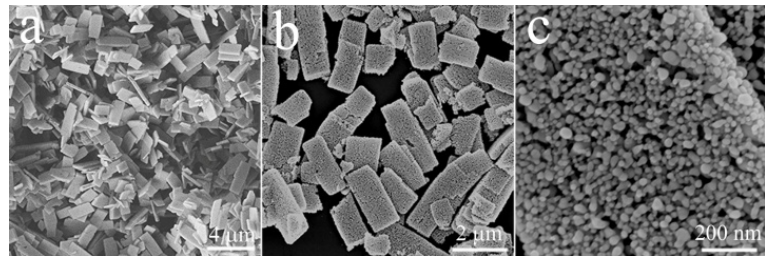


Figure S8. FE-SEM and high-magnification FE-SEM images of a) the precursors and b, c) QPP Ag (II) structures synthesized at pH= 6.0.

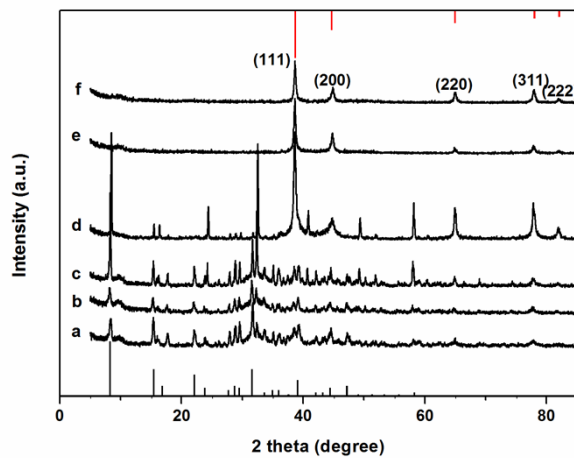


Figure S9. XRD patterns of the precursors obtained by different pH value: (a) 6.0, (b) 6.6, (c) 7.1, (d) 7.4, (e) 8.1 and (f) 8.5. The red line on the top of the frame is the standard XRD pattern of silver, the black line on the bottom the frame is the standard XRD pattern of silver citrate.

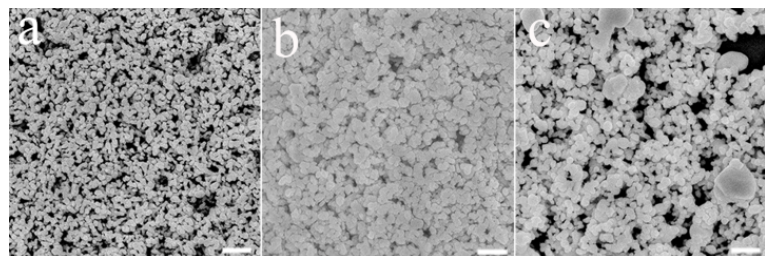


Figure S10. FE-SEM images of the product a) when pH=8.1, b) when pH=8.5 with D-glucose , and c) without D-glucose, keeping all the other experiment parameters the same as FPP Ag (I) precursor. The scale bar is 500 nm.

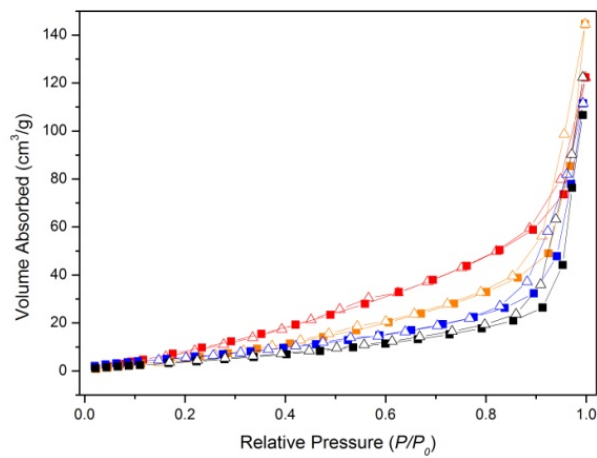


Figure S11. Nitrogen adsorption/desorption isotherms of porous Ag structures. ■=adsorption isotherms, △=desorption isotherms. FPP Ag (I) (black curve), FPP Ag (II) (blue curve), QPP Ag (I) (red curve) and QPP Ag (II) (orange curve).

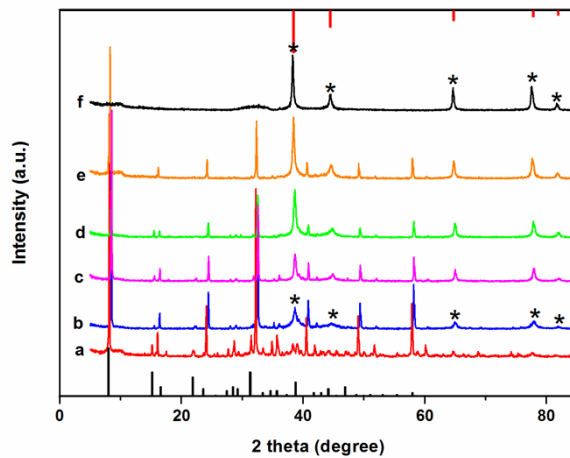


Figure S12. XRD patterns of the products in the presence of D-glucose with different aging time: a-f) 5 min, 10, 25, 40, 60 and 120 h. A group of peaks marked with * is the characteristic peaks of silver.

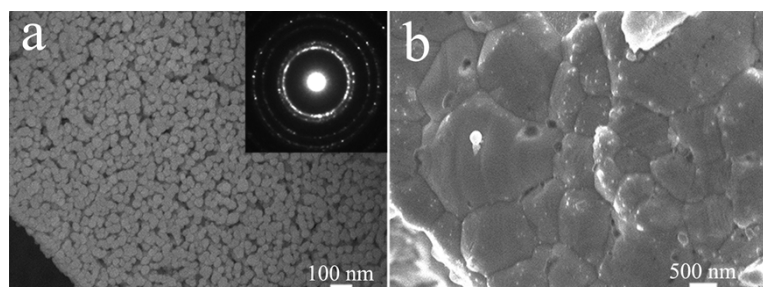


Figure S13. FE-SEM images of the cross-sectional microstructure of as-prepared porous Ag performed a) at 180 °C for 20 min at slower ($\text{ca } 2 \text{ }^{\circ}\text{C min}^{-1}$) heating rate; b) at 400 °C for 20 min at the rate of $8 \text{ }^{\circ}\text{C min}^{-1}$.

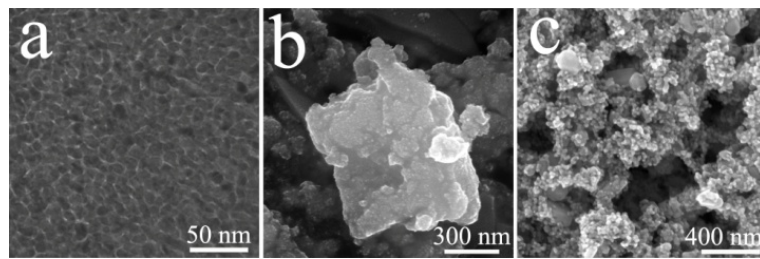


Figure S14. a) TEM image of the precursors of FPP Ag (I); b) the FE-SEM image of the as-prepared FPP Ag (I) precursors with 2h aging time; c) the FE-SEM image of the products with starch.

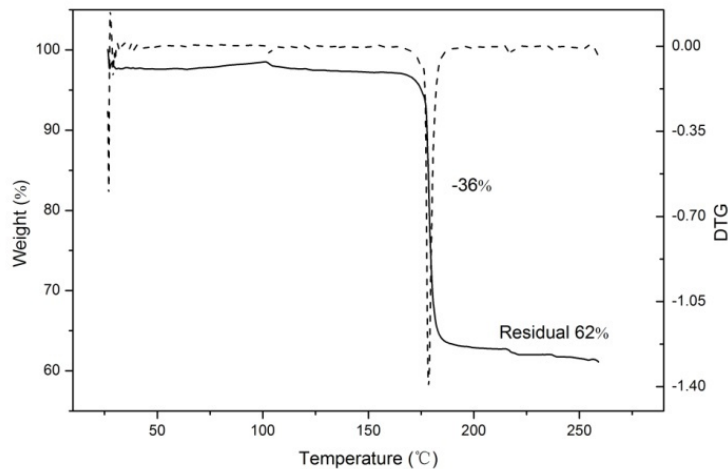


Figure S15. TG profile for the FPP Ag (I) precursor powder heated at $10\text{ }^{\circ}\text{C min}^{-1}$ at $178\text{ }^{\circ}\text{C}$.

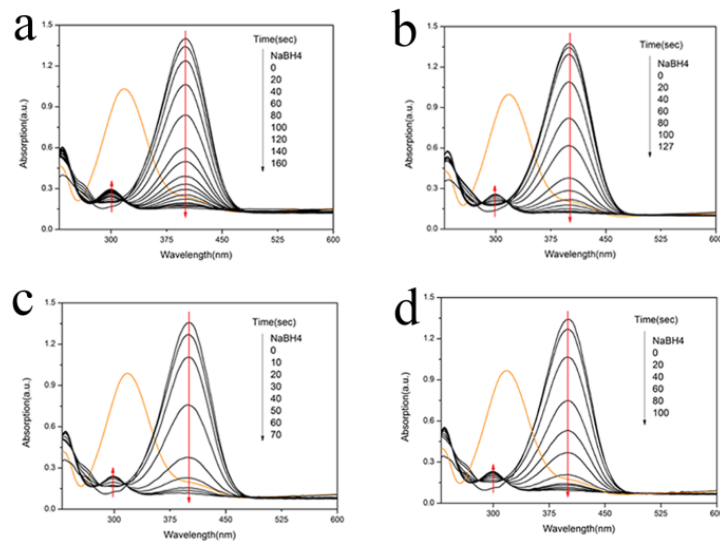


Figure S16. Successive UV-Vis spectra of reduction of *p*-nitrophenol by porous Ag structures. a) FPP Ag (I); b) FPP Ag (II); c) QPP Ag (I); d) QPP Ag (II).

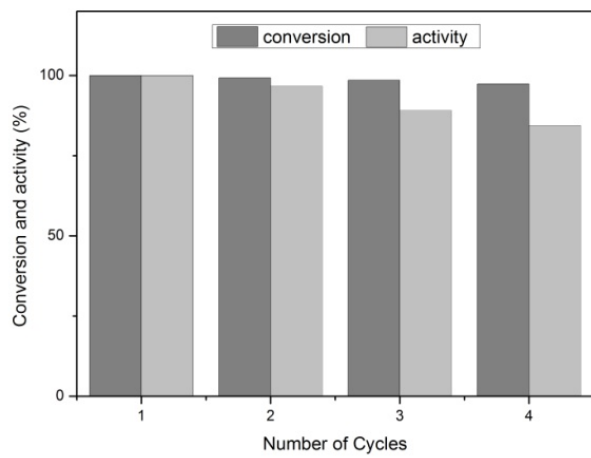


Figure S17. The change in the conversion and activity of the QPP Ag (I) with repeated usage.

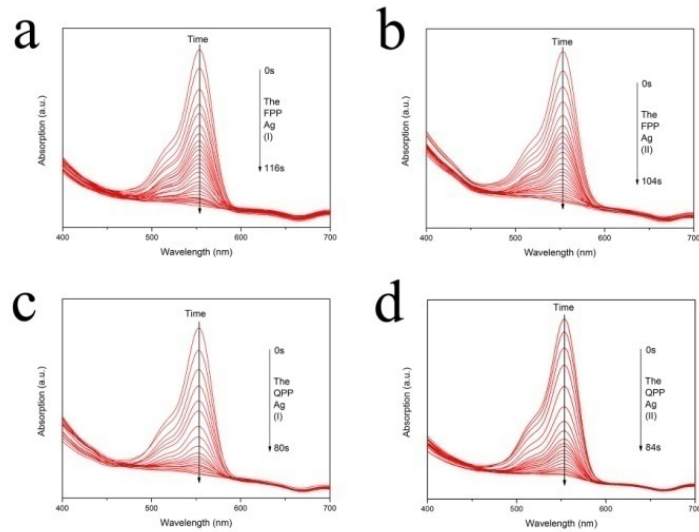


Figure S18. UV-vis absorption spectra during the catalytic degradation of Phenosafranine over time with a) FPP Ag (I); b) FPP Ag (II); c) QPP Ag (I); d) QPP Ag (II). The interval is 4s.

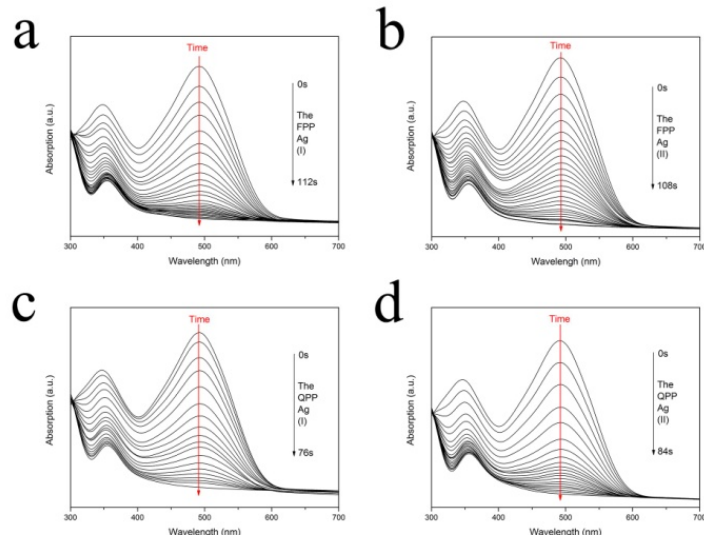


Figure S19. UV-vis absorption spectra during the catalytic degradation of Congo red over time with a) FPP Ag (I); b) FPP Ag (II); c) QPP Ag (I); d) QPP Ag (II). The interval is 4s.

Table S1. Summary of the experimental conditions and corresponding morphology of the porous Ag structures.

Sample name	The precursors (ml)				pH (ca.)	Average Length(μm)	Figure
	Na ₃ Cit	Na ₂ CO ₃	AgNO ₃	D-glucose			
FPP Ag (I)	1	1	3	4	7.4	36	1, S1
FPP Ag (II)	1	0.75	3	4	7.1	25	S7
QPP Ag (I)	1	0.5	3	4	6.6	4.0	3, S4, S5
QPP Ag (II)	1	0.25	3	4	6.0	2.5	S8

Table S2. Comparison of the rate constants for Ag crystallites from different articles.

Sample name	Rate const /K (s ⁻¹)	Reference
Silver nanodendrites	0.563×10 ⁻²	1
Corallike dendrite	0.519×10 ⁻²	2
Ag10@SBA-15	1.274×10 ⁻²	3
AgNPs/SNTs-4	3.841×10 ⁻²	4
AgNPs	0.406×10 ⁻²	5
CNFs/AgNPs composite nanofibers	0.620×10 ⁻²	6
PNIPA network and Ag nanoparticles composite	0.350×10 ⁻²	7
QPP (II) structure	6.430×10 ⁻²	This work

Supplementary References

- 1 W. Zhang, F. Tan, W. Wang, X. Qiu, X. Qiao and J. Chen, *J Hazard Mater*, 2012, **217-218**, 36-42.
- 2 M. H. Rashid and T. K. Mandal, *J. Phys. Chem. C*, 2007, **111**, 16750-16760.
- 3 B. Naik, S. Hazra, V. S. Prasad and N. N. Ghosh, *Catal Commun*, 2011, **12**, 1104-1108.
- 4 Z. Zhang, C. Shao, Y. Sun, J. Mu, M. Zhang, P. Zhang, Z. Guo, P. Liang, C. Wang and Y. Liu, *J. Mater Chem*, 2012, **22**, 1387-1395.
- 5 A. Gangula, R. Podila, R. M. L. Karanam, C. Janardhana and A. M. Rao, *Langmuir*, 2011, **27**, 15268-15274.
- 6 P. Zhang, C. Shao, Z. Zhang, M. Zhang, J. Mu, Z. Guo and Y. Liu, *Nanoscale*, 2011, **3**, 3357-3363.
- 7 Y. Lu, Y. Mei, M. Drechsler and M. Ballauff, *Angew Chem*, 2006, **45**, 813-816.